Technical Notes

TECHNICAL NOTES are short manuscripts describing new developments or important results of a preliminary nature. These Notes cannot exceed 6 manuscript pages and 3 figures; a page of text may be substituted for a figure and vice versa. After informal review by the editors, they may be published within a few months of the date of receipt. Style requirements are the same as for regular contributions (see inside back cover).

Determination of Thermal Transport Properties in Ammonium Perchlorate

John A. Stark* and R.E. Taylor†
Purdue University, West Lafayette, Indiana

Introduction

TO understand the complex combustion process in a solid rocket motor, the phenomenon must be studied on a microscopic scale at the burning surface of the propellant. Heat transmission away from the burning surface into the unburned propellant is important,[1,2] but is not well-understood. Among other shortcomings, there is a lack of reliable transport property data for propellants. It has been the purpose of this research program to measure the thermophysical properties of and study the nature of heat transfer through ammonium perchlorate (AP). Specifically, the properties of interest here are thermal diffusivity and thermal conductivity. Specific heat results are presented elsewhere.[3]

AP has two solid-state phases important to rocket applications. Phase II exists from −190 to 240°C; its crystal lattice is orthorhombic. Phase III exists from 240 to 450°C (the melting point); its lattice is cubic. Significant decomposition of AP begins around 202°C.[4]

Method

The flash technique[5] was used to measure diffusivity. Application of this method is described thoroughly by Taylor.[6] The flash method involves a thin, disk-shaped sample flashed with a short-duration laser pulse on its front face. The rear-face temperature-rise history is then recorded. To safely allow maximum absorptance of the laser energy on the front face, it was decided that AP would be the rear layer of a two-layer sample, and be glued to a front layer of either stainless steel or graphite. Data analysis was accomplished by the method described by Stark.[7] This method accounts for the presence of heat loss in two-layer samples of the type used.

An In-Sb i.r. detector was used to measure the rear-surface temperature. To ensure that only the rear surfaces were seen, they were covered with a thin layer of black enamel paint. It was shown that this layer of paint was thin enough not to affect the diffusivity measurements significantly.

Because of the expected anisotropy of AP crystals, it was desirable to obtain diffusivity values along each of the crystallographic axes. Several single crystals of 99.999% pure AP were acquired from the Naval Weapons Center. These crystals were large enough to allow cleavage of several diffusivity samples from each. Since cleavage of an AP crystal along planes perpendicular to each of its crystallographic axes is not easily accomplished, the cleavage planes used were those parallel to the natural growth surfaces of the crystal; these are the Miller planes ⟨002⟩, ⟨210⟩, and ⟨2$\bar{1}$0⟩. In the diffusivity samples these planes were made parallel to the sample faces. Therefore, diffusivities were measured perpendicular to the indicated Miller planes.

The ⟨002⟩ measurements were parallel to the crystallographic *c* axis. The ⟨210⟩ and ⟨2$\bar{1}$0⟩ measurements were in the directions that lay in the *a-b* plane. Due to the symmetry of these two directions through the crystal structure, the diffusivities were expected to be the same. The set of two equations needed to resolve the diffusivities along the *a* and *b* axes became singular and could not be solved. Therefore, results are reported as diffusivities perpendicular to the cleavage planes, rather than parallel to the *a* and *b* axes. Since all of the large AP crystals were of the same shape, and they appeared similar to crystals studied by Kraeutle,[8] all of the crystals were expected to have the same lattice orientation in relation to their observed shape. One of the large crystals was used for x-ray-induced lattice defects.[9] Therefore, the other crystals were used to make diffusivity samples. In addition, the thermal diffusivities of various mixtures of AP granules and hydroxy-terminated polybutadiene (HTPB) binder were measured and conductivity values for the mixtures and pure AP were calculated.

Results and Discussion

Diffusivity curves for each of the three AP crystal directions are shown in Fig. 1 along with the data for a decomposed sample in the high-temperature, cubic phase. The curves for orthorhombic ⟨210⟩ and ⟨2$\bar{1}$0⟩ data are very similar. This was expected because of the symmetry of these directions through the crystal lattice. It may also be noted that the ⟨00$\bar{2}$⟩ results have about the same magnitude as the ⟨210⟩ and ⟨2$\bar{1}$0⟩ data.

In light of the susceptibility of AP to damage by x rays, lattice defects were probably present on a large enough scale to be an important effect on the phonon transfer mechanism. Numerous defects would increase phonon scattering, thus reducing the conductivity below that which would be observed in a perfect crystal. Defect presence may also account for some of the variation between samples. When cleaving the crystals, small cleavage steps or surface cracks would often appear on the sample. Sample-to-sample discrepancies were also probably due to errors caused by interlayer contact resistance. Although not strongly present in the crystal samples, it was probably different in each sample.

The diffusivity values of AP-HTPB binder samples with various percentages of AP are shown in Fig. 2. Notice that the pure binder diffusivity is much lower than that of the AP single crystal. As expected, the addition of AP to the binder can be seen to increase the diffusivity of the mixture.

Bulk conductivity values for the AP binder samples were calculated using the diffusivities from Fig. 2 and specific heat values from Ref. 3. Since the AP granules were much smaller than the sample rear-layer thickness, the mixture can be treated as macroscopically homogeneous to enable calculation of these effective bulk conductivities, which represent only the precise mixtures measured.

To obtain pure AP conductivities from the mixture data available, an equation was required which relates the conductivities of each of the two strictly homogeneous phases in a mixture to the bulk conductivity of the mixture. The Russell

Submitted July 17, 1984; revision submitted April 18, 1985.

*Graduate Student, Thermophysical Properties Research Laboratory, School of Mechanical Engineering. Member AIAA.

†Senior Researcher and Director, Thermophysical Properties Research Laboratory.

equation was shown by Cheng and Vachon[10] to predict well the measurements of mixtures similar to the AP binder samples studied here. This model assumes that one of the two phases present is continuous, and the other is made up of discrete particles dispersed throughout the continuous medium. The Russell equation is

$$k_m = k_c \frac{P_d^{2/3} + (k_c/k_d)(1-P_d^{2/3})}{P_d^{2/3} - P_d + (k_c/k_d)(P_d + P_d^{2/3})} \quad (1)$$

In applying Eq. (1) to the AP binder samples, k_m was the measured value, k_c the binder conductivity (assumed to be constant at 0.00202 W/cm-K), and k_d the unknown AP crystal conductivity. An iterative solution was implemented that provided the results shown in Fig. 3 as pure crystal conductivities (average values for random directions through the crystal). Samples with AP mass fractions between 70 and 85% provided about the same curve of calculated pure AP conductivity.

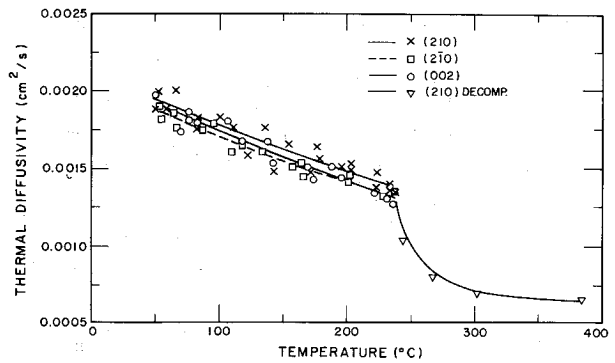

Fig. 1 Measured diffusivities of AP single crystal.

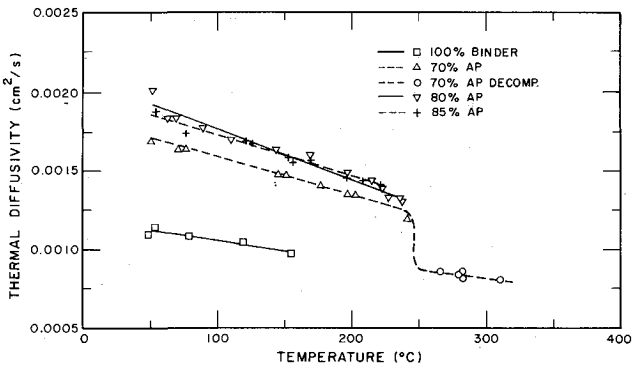

Fig. 2 Measured diffusivities of AP binder mixtures and AP powder.

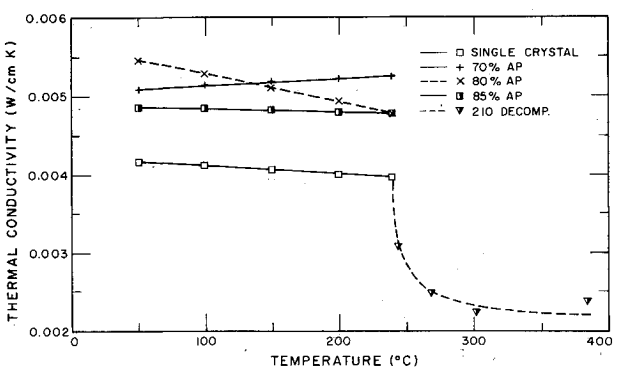

Fig. 3 AP conductivity results.

Figure 3 is a summary of all of the conductivity values presented. All of these curves represent values for pure, solid AP; that is, the binder and powder sample data have been corrected for the presence of a second phase. The difference between the conductivity values for AP calculated from AP binder data and the actual single crystal data can be explained. It is probable that the single crystals had significant structural imperfections, yet the very small crystal grains in the binder samples may have been relatively free of internal imperfections. This situation would imply a significantly larger phonon-imperfection scattering in the single crystal samples than in the AP grain of the binder samples, thus producing lower conductivities in the former.

It can be concluded that there is very little anisotropy in the transport properties in AP. The error of the diffusivity data presented here is estimated to be within ±14% in any direction. Through the study of AP binder mixtures, bulk conductivity values can be predicted for any typical propellant mixtures of these two materials.

The data presented have application in the modeling of rocket motor combustion phenomena. Although the temperatures at which properties were measured are not comparable to combustion surface temperatures, the values given are very indicative of those expected at the combustion temperatures. As dielectrics, these materials have conductivities that tend to decrease with increasing temperature. The present work shows that the temperature dependencies of conductivities of the materials are small. Therefore, the data given represent an upper bound on values expected at combustion temperatures. Upon decomposition or solid-phase change the conductivity values will decrease as shown, after which time they can be expected to remain nearly constant due to the very limited order in the material structure. This reasoning puts a lower bound on the values at combustion temperature. This lower bound is represented by decomposed AP crystals (Fig. 3).

Acknowledgments

The authors are indebted to Ms. Leslie G. Koshigoe for the measurement of AP specific heat. Thanks are also extended to Dr. Thomas Boggs, Dr. G.L. Liedl, Mr. Robert Askins, and the Thermophysical Properties Research Laboratory staff. This research was funded by the Air Force Office of Scientific Research, Dr. L.H. Caveny, project monitor.

References

[1]Cohen, N.S., "Response Function Theories that Account for Size Distribution Effect—A Review," *AIAA Journal*, Vol. 19, July 1981, pp. 907-912.

[2]Imber, M., "Thermal Conductivity: A Parameter in Solid Propellant Burning," *AIAA Journal*, Vol. 4, Sept. 1966, pp. 1610-1617.

[3]Shoemaker, R.L., Stark, J.A., and Taylor, R.E., "Thermophysical Properties of Propellants," *Proceedings of the 8th European Thermophysical Properties Conference*, Manchester, UK, 1984, also *High Temperatures-High Pressures*, in press.

[4]Brill, T.B. and Goetz, F., "Laser Raman Study of the Thermal Decomposition of Solid NH_4ClO_4," *Journal of Chemical Physics*, Vol. 65, Aug 1976, pp. 1217-1219.

[5]Parker, W.J., Jenkins, R.J., Butler, C.P., and Abbott, G.L., "Flash Method of Determining Thermal Diffusivity, Heat Capacity and Thermal Conductivity," *Journal of Applied Physics*, Vol. 32, No. 9, Sept. 1961, pp. 1679-1684.

[6]Taylor, R.E., "Heat-Pulse Thermal Diffusivity Measurements," *High Temperatures-High Pressures*, Vol. 11, 1979, pp. 43-58.

[7]Stark, J.A., "Measurement of Thermal Transport Properties of Selected Solid Rocket Propellant Components," Master's Thesis, School of Mechanical Engineering, Purdue University, W. Lafayette, Ind., Aug. 1984.

[8]Kraeutle, K.J., "The Thermal Decomposition of Orthorhombic Ammonium Perchlorate Single Crystals," *Journal of Physical Chemistry*, Vol. 74, March 1970, pp. 1350-1356.

[9]Jacobs, P.W.M. and Pearson, G.S., "Mechanism of the Decomposition of Ammonium Perchlorate," *Combustion and Flame*, Vol. 13, Aug. 1969, pp. 419-443.

[10]Cheng, S.C. and Vachon, P.I., "A Technique for Predicting the Thermal Conductivity of Suspension, Emulsions, and Porous Materials," *International Journal of Heat and Mass Transfer*, Vol. 13, March 1970, pp. 537-546.

Criteria for the Evaluation of Laser Solar Energy Converter Systems

W.L. Harries*
Old Dominion University, Norfolk, Virginia

I. Introduction

ONE concept for collecting solar energy is to use large solar collectors on orbiting space stations, which then transmit the energy as laser beams. Direct conversion by solar pumped gas lasers has already been considered and the power conversion efficiency disscussed.[1-3] However, a figure of merit, of more importance for space missions, is the output power per unit weight ratio.

An idealized energy conversion system is shown in Fig. 1. The solar radiance is collected in a parabolic reflector and, for a required output power, its area is determined by the laser efficiency. The power not converted into the laser beam must be dissipated by a heat radiator emitting by Stefan's Law which, as the converter efficiency is usually low, will contribute the major part of the total weight of the system.

The overall efficiency of the laser can be decomposed into the product of several efficiencies, which affect the collector and radiator in different ways. The efficiencies are described in Sec. II and the energy flow is discussed in Sec. III. The dependencies of weight on area are then assumed, which determine the weight for a given output power. Some comparisons will be shown of different laser systems.

II. Efficiency of Solar Pumped Lasers

The overall efficiency of solar pumped lasers can be subdivided into the product of four efficiencies.[1] First, it aborption occurs over a bandwidth λ_1 to λ_2, the fraction of the solar spectrum used, or "solar utilization efficiency," is η_S,

$$\eta_S = \int_{\lambda_1}^{\lambda_2} \Phi(\lambda)\mathrm{d}\lambda \Big/ \int_0^{\infty} \Phi(\lambda)\mathrm{d}\lambda$$

where $\Phi(\lambda)$ is the solar radiance in photons per square meter between λ and $\lambda + \mathrm{d}\lambda$.

The absorption efficiency η_A is that fraction of photons within the absorption bandwidth absorbed by the gas: $\eta_A = 1 - \exp(-\sigma_a(N)\mathrm{d})$, where σ_a is the absorption cross section, (N) the density of absorbers, and d the thickness of gas.

Of the photons absorbed, only a fraction, η_K, end up producing a lasing transition. The kinetic efficiency η_K is determined by the detailed kinetics of the laser and, for example, it takes accounts of losses in the upper laser level due to quenching, etc.[2,3] Finally, the quantum efficiency η_Q is the ratio of the energy of the emitted photon to the average energy of the absorbed photons.

The device efficiency would then be $\eta_D = \eta_A\eta_K\eta_Q$, and the overall solar efficiency $\eta = \eta_S\eta_A\eta_K\eta_Q$, which is usually an order of magnitude less than η_D.

Received Nov. 20, 1984; Technical Note received April 22, 1985.

*Professor, Department of Physics.

III. Energy Flow in Solar Pumped Lasers

The energy flow for the idealized model in Fig. 1 is shown in Fig. 2. The solar power falling on the collector of area A_c is P_i. The mirror of reflectivity r concentrates the flux, and a fraction rP_i reaches the first transparent wall containing the lasing medium. However, a fraction $(1-r)P_i$ has been absorbed by the mirror and has to be radiated. The first container wall is assumed to have a transmittance τ_1, so the power arriving at the lasing medium is $\tau_1 rP_i$, and the power absorbed by the wall is $(1-\tau_1)rP_1$, which also has to be radiated.

The power arriving at the laser medium is distributed in wavelength over the solar spectrum; only a fraction, η_S, can be utilized, and of that only η_A is absorbed. The power absorbed P_A is $\eta_S\eta_A\tau_1 rP_i$ and the output power P_O is $\eta_K\eta_Q P_A$, while the part lost due to the lasing process, $(1-\eta_K\eta_Q)P_A$, has to be radiated. The power not absorbed by the lasing medium is $(1-\eta_S\eta_A)\tau_1 rP_i$ and reaches the second wall of transmittance τ_2. Then $\tau_2(1-\eta_S\eta_A)\tau_1 rP_i$ is transmitted through it, but an amount $(1-\tau_2)(1-\eta_S\eta_A)\tau_1 rP_i$ absorbed in the wall has to be radiated.

The total power that has to be radiated is P_r

$$P_r = P_i\{(1-r) + r(1-\tau_1) + r\tau_1\eta_S\eta_A(1-\eta_K\eta_Q) + r\tau_1(1-\eta_S\eta_A)(1-\tau_2)\} \quad (1)$$

As the output power P_O and input power P_i are related by $P_O = r\tau_1\eta P_i$, the relation between the radiated and output power is

$$P_r = KP_O/\eta \quad (2)$$

where

$$K = (1/r\tau_1)[(1-r) + r(1-\tau_1) + r\tau_1\eta_S\eta_A(1-\eta_K\eta_Q) + r\tau_1(1-\tau_2)(1-\eta_S\eta_A)] \quad (3)$$

IV. Output Power to Weight Ratio

The solar irradiance I_0 is 1.4 KWm^{-2}, and if the output power is $P_O(kW)$, then the area of the collector $A_c(m^2)$ *is*

$$A_c = P_O/(I_0\eta r\tau_1) \quad (4)$$

The radiator emits by Stefan's Law and its area is

$$A_r = P_r/\sigma\epsilon T^4 \quad (5)$$

where σ is Stefan's constant, ϵ the emissivity, and T, the temperature of the emitting surface. It is assumed that efficient conduction by heat pipes causes T to approach the work-

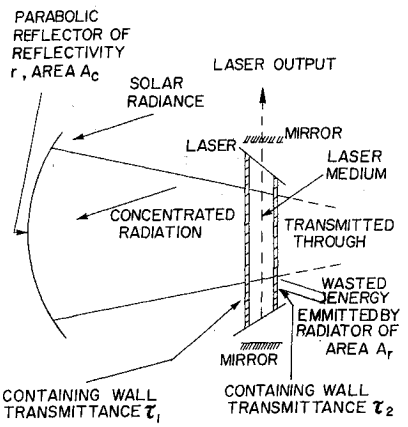

Fig. 1 Idealized arrangement for a solar pumped laser.